

NPS ARCHIVE  
1959  
ARN, R.

THE BEHAVIOR OF STAINLESS STEEL  
UNDER EXPLOSIVE LOADS  
AT VARIOUS TEMPERATURES

---

ROBERT W. ARN  
AND  
GERALD C. CANAAN

LIBRARY  
U.S. NAVAL POSTGRADUATE SCHOOL  
MONTEREY, CALIFORNIA

DUDLEY KNOX LIBRARY  
NAVAL POSTGRADUATE SCHOOL  
MONTEREY, CA 93943-5101









THE BEHAVIOR OF STAINLESS STEEL  
UNDER EXPLOSIVE LOADS AT VARIOUS TEMPERATURES

\* \* \* \* \*

Robert W. Arn  
and  
Gerald C. Canaan





THE BEHAVIOR OF STAINLESS STEEL  
UNDER EXPLOSIVE LOADS AT VARIOUS TEMPERATURES

by

Robert W. Arn

Lieutenant, United States Navy

and

Gerald C. Canaan

Lieutenant, United States Navy

Submitted in partial fulfillment of  
the requirements for the degree of

MASTER OF SCIENCE  
IN  
ELECTRICAL ENGINEERING

United States Naval Postgraduate School  
Monterey, California

1 9 5 9

Thesis

W. S.

NPS ARCHIVE

1959

ARL, R.

DUDLEY KNOX LIBRARY  
NAVAL POSTGRADUATE SCHOOL  
MONTEREY, CA 93943-5101

THE BEHAVIOR OF STAINLESS STEEL  
UNDER EXPLOSIVE LOADS AT VARIOUS TEMPERATURES

by

Robert W. Arn

and

Gerald C. Canaan

This work is accepted as fulfilling  
the thesis requirements for the degree of

MASTER OF SCIENCE

IN

ELECTRICAL ENGINEERING

from the

United States Naval Postgraduate School



## ABSTRACT

The use of stainless steel in various aspects of our present day technology is increasing rapidly. Its application to aircraft, missiles and satellites is of special importance to the military. In present and future applications of stainless steel, unconventional structural loading may be applied, such as bullet impact, meteorite collision and events of high intensity but of short duration. These events may be defined, generally, as impact, impulsive, and explosive loads. A study of the behavior of metals under such conditions, while not completely new, has recently been accelerated and modern analytical methods can be applied. Previous investigators have established that phase changes can and do occur during the short time intervals in which the explosive loads are applied.<sup>1,2,3,4</sup>

It is the purpose of this paper to investigate microstructural changes in stainless steel when it is subjected to an explosive load at various temperatures. It has been shown that cold working stainless steel (18% Ni, 8% Cr)

<sup>1</sup>E. W. LaRocca, Phase Transformations in the Microstructure of Explosively Loaded Iron and Steel, Bulletin of the American Physical Society, 30, pp. 16, Dec., 1955

<sup>2</sup>Samuel Katz, Deformation Zones Produced by Explosive Shocks in Ferrous Metals, Bulletin of the American Physical Society, 30, pp. 16-17, Dec., 1955

<sup>3</sup>E. W. LaRocca and L. A. Burkardt, Effect of Impulsive Loads on the Structure of Cobalt, Bulletin of the American Physical Society, 2, pp. 263, June, 1957

<sup>4</sup>Cyril S. Smith, Microstructure of Metals Subjected to Intensive Plane Shock Waves, Journal of Metals, 10, pp. 94, Feb., 1958





reduces the austenitic structure to ferrite.<sup>5,6</sup> Wulff and his collaborators determined this phase transformation from the study of polishing and grinding effects which limited the transformation to about  $6 \times 10^{-4}$  cm. below the surface. However, this transformation was a relatively slow process which occurred after extensive grinding and polishing. The investigation as described in this report will indicate that it is possible to obtain similar structural changes during time intervals of ten to fifty microseconds.

Conventionally, any phase formed by a shear mechanism is called martensitic, and in steel the structure is a body-centered tetragonal.<sup>7</sup> However, with low carbon content, tetragonality disappears, and the martensite formed will be essentially a body-centered cube.<sup>8</sup> In iron, ferrite is the body-centered cubic phase, and the word ferrite in this report is used to designate that product of the transition of the austenite in type 304 stainless steel.

This work was done at the U. S. Naval Ordnance Test Station, China Lake, California. The authors wish to express their appreciation to Mr. John Pearson and especially to Mr. E. W. LaRocca who gave so freely of his time and knowledge which helped considerably in this project.

<sup>5</sup>J. Wulff, Trans. AIME, Vol. 145, pp. 295, 1941

<sup>6</sup>J. T. Burwell and J. Wulff, Trans. AIME, Vol. 135, pp. 486, 1939

<sup>7</sup>C. S. Barrett, Structure of Metals, pp. 560, McGraw-Hill Book Co., Inc., 1952

<sup>8</sup>E. O. Hall, Twinning and Diffusionless Transformations in Metals, pp. 124-138, Butterworths Scientific Publications, 1954



## TABLE OF CONTENTS

Section	Title	Page
1.	Introduction	1
2.	Sample Preparation	2
3.	Equipment	7
4.	Polishing Technique	8
5.	Discussion of Microstructures	10
6.	Discussion of X-Ray Structures	18
7.	Hardness	32
8.	Conclusions	34
9.	Bibliography	35
10.	Appendix I	37
11.	Appendix II	38
12.	Appendix III	39



# LIST OF ILLUSTRATIONS

Figure	Title	Page
1.	Diagram of Explosive Press	3
2.	Detonated Sample after Polishing and Etching	9
3.	Grain Structure of Sample Annealed for One Hour, 200X	11
4.	Grain Structure of Sample Loaded at $\nearrow 97^{\circ}\text{C.}$ , Unloaded End, 200X	12
5.	Grain Structure of Sample Loaded at $\nearrow 97^{\circ}\text{C.}$ , Loaded End, 200X	12
6.	Grain Structure of Sample Loaded at $\nearrow 20^{\circ}\text{C.}$ , Unloaded End, 200X	14
7.	Grain Structure of Sample Loaded at $\nearrow 20^{\circ}\text{C.}$ , Loaded End, 200X	14
8.	Grain Structure of Sample Loaded at $- 190^{\circ}\text{C.}$ , Unloaded End, 200X	15
9.	Grain Structure of Sample Loaded at $- 190^{\circ}\text{C.}$ , Loaded End, 200X	15
10.	Grain Structure of Sample Loaded at $- 190^{\circ}\text{C.}$ , Unloaded End, 1500X	16
11.	X-ray Diffraction of Sample Annealed for One Hour	24
12.	X-ray Diffraction, Loaded and Unloaded Ends, of Sample Loaded at $\nearrow 97^{\circ}\text{C.}$	24
13.	X-ray Diffraction, Loaded and Unloaded Ends, of Sample Loaded at $\nearrow 20^{\circ}\text{C.}$	25
14.	X-ray Diffraction, Loaded and Unloaded Ends, of Sample Loaded at $- 190^{\circ}\text{C.}$	27
15.	X-Ray Diffraction in Quadrant Form of Samples Annealed, Loaded at $- 190^{\circ}\text{C.}$ , $\nearrow 97^{\circ}\text{C.}$ and $\nearrow 20^{\circ}\text{C.}$ marked 1, 2, 3 and 4 respectively.	29
16.	X-ray Diffraction in Quadrant Form of Samples of Annealed Iron, Loaded at $\nearrow 97^{\circ}\text{C.}$ , $\nearrow 20^{\circ}\text{C.}$ and $- 190^{\circ}\text{C.}$ marked 1, 2, 3 and 4 respectively.	30
17.	Hardness Versus Distance From The Loaded End For Each Sample	33





## TABLE OF DEFINITIONS

- alpha iron.** The form of iron that is stable below 910 C and characterized by a body-centered cubic crystal structure.
- annealing.** A heat treatment designed to effect softening of a coldworked structure by re-crystallization or grain growth or both.
- austenite.** A solid solution in which gamma iron is the solvent; characterized by a face-centered cubic crystal structure.
- back reflection.** X-ray diffraction at deviations near 180 degrees, especially useful in precise measurement of interplanar distances.
- body-centered.** Having the equivalent lattice points at the corners of a unit cell, and at its center.
- cold working.** Deforming a metal plastically at such a temperature and rate that strain hardening occurs.
- collimate.** To isolate a parallel, or nearly parallel, beam of rays, as by slits, pinholes or a channel.
- crystal.** A coherent piece of matter all parts of which have the same anisotropic arrangement of atoms in metals, usually synonymous with grain and crystallite.
- diffraction.** The deviation of an X-ray beam by scattering from atoms that have some regularity of arrangement or spacing.
- face-centered.** Having equivalent points at the corners of the unit cell and at the centers of its six faces.
- ferrite.** A solid solution in which alpha iron is the solvent and which is characterized by a body-centered cubic crystal structure.
- focusing.** Using such a shape and position of sample and position of source that the diffracted X-rays from many or all parts of the sample fall close together in the diffraction pattern. Such methods permit the use of wide beams and require relatively short exposures.
- gamma iron.** The form of iron stable between 910 C. and 1400 C. and characterized by a face-centered cubic crystal structure.
- grains.** Individual crystals in metals.



**martensite.** An unstable constituent in quenched steel, formed without diffusion and only during cooling below a certain temperature known as the temperature at which transformation of austenite to martensite starts during cooling. Tetragonality of the crystal structure is observed when the carbon content is greater than about 0.5%

**metallography.** The science concerning the constitution and structure of metals and alloys as revealed by the microscope.

**metastable.** A tendency to change into a stable form if conditions are provided.

**Miller indices.** The smallest integers proportional to the reciprocals of the intercepts, in terms of the parameters (a,b,c,) of the plane on the three crystal axes; written, in general (hkl); in particular, for example (110).

**micron.** A linear distance of 0.001 mm.

**polycrystalline.** Consisting of more than one crystal.

**powder method (for X-ray analysis).** A method using a loose aggregate of small crystals with chaotic orientation; Debye-Scherrer method, Hull method.

**preferred orientation.** In a polycrystalline structure, a departure from crystallographic randomness.

**quenching.** A process of rapid cooling from an elevated temperature by contact with liquids, gases or solids.

**reflection (X-ray).** Diffraction considered to result from scattering by crystal planes as units. These are the reflecting planes. Monochromatic X-rays are reflected in accordance with Bragg's Law.

**scattering (fluorescence).** The re-emission of X-rays from irradiated matter, without change of wave length; scattering takes place in all directions with respect to the incident X-rays, but more intensely in some direction than in others.

**target.** The part of the anti-cathode wholly or predominantly of a single metal, where the focus lies.

**tetragonal.** Having 4-fold axes of symmetry but no 3-fold axes of symmetry. The typical tetragonal crystal has two equal axes (b = a) perpendicular to each other and to a third axis (c).

**Vickers hardness test.** An indentation hardness test employing a 136 degree diamond pyramid indenter and variable



loads enabling the use of one hardness scale.

X-rays. Light rays excited usually by the impact of cathode rays on matter, which have wave lengths between  $10^{-6}$  cm. and  $10^{-9}$  cm.





## 1. Introduction

A selected rod of low carbon, 18-8 stainless steel was cut into  $\frac{1}{2}$  inch lengths and annealed. These pieces of stainless steel were subjected to an explosive load using tetryl as the explosive. This load was imposed at temperatures of  $+97^{\circ}\text{C}$ ,  $+20^{\circ}\text{C}$  and  $-190^{\circ}\text{C}$ . Inasmuch as the load and rate of application of the load were considered constant in each case, the primary variable was that of temperature.

Each sample, after having been loaded, was polished, etched and examined at a magnification of 200x. In particular, comparisons were made between the detonated and undetonated ends. Pictures of the crystal structure taken of each sample are included in the body of the report.

After explosive loading, it was noted that the samples, previously non-magnetic, showed an attraction to a magnet, indicating a change of phase or crystal structure. The next step was to verify that a phase change had occurred and this was done using back reflection X-ray diffraction techniques. Pictures of the diffraction patterns obtained in each case are also included in the body of the report. The microhardness versus distance from the impacted end for each sample was also investigated.



## 2. Sample Preparation

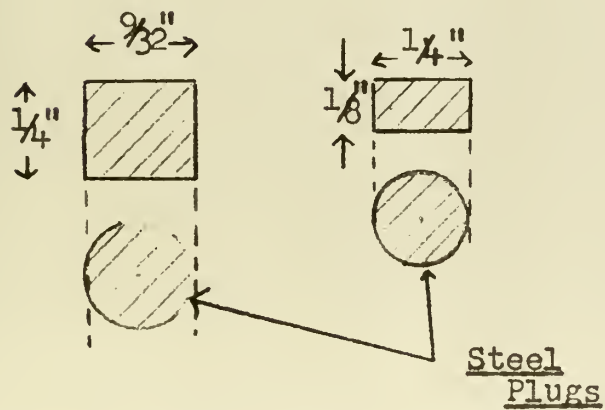
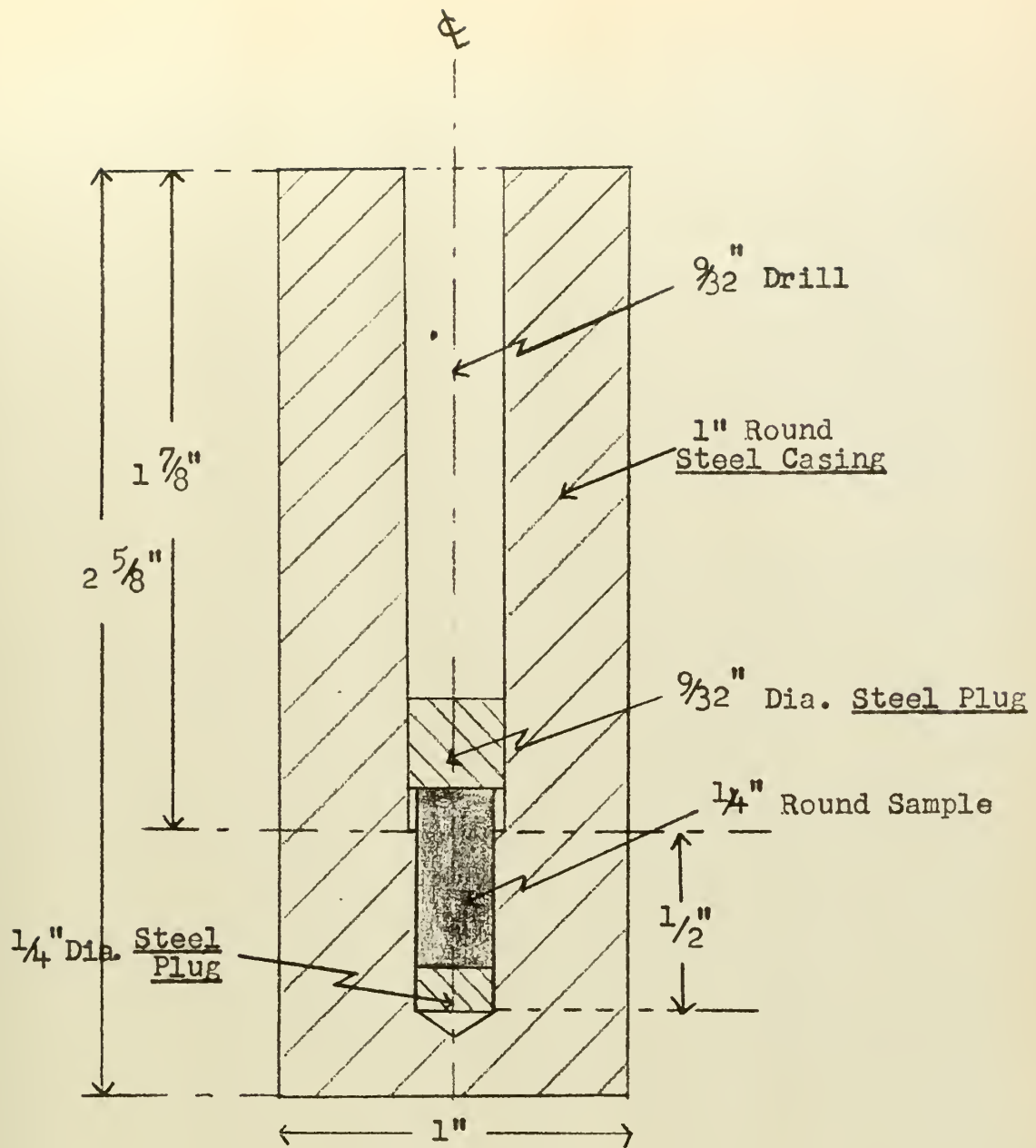
The stainless steel specimen used for this investigation was type 304. All samples were cut from the same piece of  $\frac{1}{4}$  inch rod. A certificate of analysis together with pertinent mechanical properties is contained in Appendix I.

Three  $\frac{1}{2}$  inch long samples were cut and annealed for periods of one, two and three hours in an electric oven at 1050°C. Each sample was water quenched to 13°C immediately upon removal from the furnace. Microscopic examination of these three samples revealed that annealing for one hour at 1050°C was sufficient to remove the effects of original cold work and relieve induced strains. Little or no grain growth was noted, while oxidation effects increased significantly as annealing time increased to three hours. On the basis of this preliminary investigation it was decided that an annealing time of one hour was sufficient to insure a homogeneous, austenitic structure for future sample preparation.

Nine samples  $\frac{1}{4}$  inch by  $\frac{1}{2}$  inch were then annealed as described previously and subjected to impulsive loading at the temperatures of  $+97^{\circ}\text{C}$ ,  $+20^{\circ}\text{C}$  and  $-190^{\circ}\text{C}$ .

Fig. 1 is a scale drawing of the explosive press used for this investigation. This press was designed by E. W. LaRocca of the U.S. Naval Ordnance Test Station, China Lake, California. The press was designed for applying limited compression to the sample. Drills of  $\frac{1}{4}$  inch and  $9/32$  inch were used in the press construction. This difference of  $1/32$  inch bore diameter acted as a stop for the upper steel plug and this limited the compression stroke to  $1/8$  inch or





EXPLOSIVE PRESS

Scale 2: 1

Fig. 1





approximately  $\frac{1}{4}$  the length of the test sample.

The explosive train consisted of a DuPont Engineers Special detonator and a  $\frac{1}{4}$  inch by  $\frac{1}{4}$  inch tetryl pellet. The detonation proceeded high order at all three temperatures, characterized by a very high rate of reaction and high pressure. Detonation rates of the order of 25,000 feet per second and an instantaneous pressure rise of  $3 \times 10^6$  pounds per square inch acting for a total duration of less than 50 microseconds were expected.<sup>9</sup>

Three of the samples were impulsively loaded with the samples and presses elevated to a temperature of  $\nearrow 97^{\circ}\text{C}$ , achieved by immersing the entire system in boiling water. For each of the three firings at this temperature, the presses were plastically deformed at the centers but still intact. The test samples were recovered by machining the press free of the sample. The next three samples of the test series were explosively loaded at ambient temperature which was  $\nearrow 20^{\circ}\text{C}$ . In each of the three firings the presses were fractured lengthwise into four main sections. The samples, in each case, were recovered intact. The final three samples were explosively loaded at a temperatures of  $- 190^{\circ}\text{C}$ , attained by immersing the entire system in liquid nitrogen until temperature equilibrium was reached. In each case, upon detonation, the presses were fractured severely into many small pieces. Each of the samples was recovered intact.

<sup>9</sup>John S. Rinehart and John Pearson, Behavior of Metals Under Impulsive Loads, pp. 45-63, The American Society For Metals, 1954



A careful investigation revealed that the steel end-plugs used in the press had prevented fracture of the sample in every case.

The physical dimensions of each sample were measured before and after impulsive loading and are recorded in Table 1. The percent increase in maximum and minimum cross section area were computed and found to be quite constant over the temperature range.



TABLE I  
SAMPLE DIMENSIONS

1. BEFORE DETONATION

<u>SAMPLE</u>	<u>DIAMETER</u>	<u>LENGTH</u>	<u>CROSS-SECTION AREA</u>
all	0.250 in.	0.500 in.	0.0491 sq. in.

2. AFTER DETONATION

<u>SAMPLE</u>	<u>TEMP.</u>	<u>MAX. DIA.</u>	<u>MIN. DIA.</u>	<u>LENGTH</u>
1	✓20 C.	0.292 in.	0.256 in.	0.444 in.
2	✓20 C.	0.291 in.	0.255 in.	0.458 in.
3	✓20 C.	0.292 in.	0.257 in.	0.458 in.

AV. DIA.	0.2917 in.	0.2560 in.
AV.X-SECT. AREA	0.0668 sq. in.	0.0515 sq. in.
% INCREASE AREA	36.05	4.89

<u>SAMPLE</u>	<u>TEMP.</u>	<u>MAX. DIA.</u>	<u>MIN. DIA.</u>	<u>LENGTH</u>
4	✓97 C.	0.295 in.	0.259 in.	0.438 in.
5	✓97 C.	0.295 in.	0.255 in.	0.441 in.
6	✓97 C.	0.291 in.	0.257 in.	0.446 in.

AV. DIA.	0.2937 in.	0.2570 in.
AV.X-SECT. AREA	0.0677 sq. in.	0.0517 sq. in.
% INCREASE AREA	37.88	5.30

<u>SAMPLE</u>	<u>TEMP.</u>	<u>MAX. DIA.</u>	<u>MIN. DIA.</u>	<u>LENGTH</u>
7	-190 C.	0.289 in.	0.268 in.	0.442 in.
8	-190 C.	0.298 in.	0.267 in.	0.436 in.
9	-190 C.	0.298 in.	0.265 in.	0.438 in.

AV. DIA.	0.2950 in.	0.2667 in.
AV.X-SECT. AREA	0.0684 sq. in.	0.0559 sq. in.
% INCREASE AREA	39.31	13.85



### 3. Equipment

Standard metallographic grinding papers and polishing wheels were used during sample preparation. All microstructure photographs were made using an American Optical Research Metallograph, model 2400. X-ray diffraction was accomplished using either a Hilger Research X-ray diffraction unit or by using Philips Electronic unit. Hardness tests were conducted using the American Optical Metallograph together with the Bergsman Microhardness Tester. E. W. LaRocca has adapted these instruments to each other.<sup>10</sup>

<sup>10</sup>E. W. LaRocca, Adaptation of Bergsman Microhardness Tester to American Optical Metallograph, The Review of Scientific Instruments, Vol. 26, No. 6, pp. 590-591, June, 1955





#### 4. Polishing Technique

The technique for polishing 18-8 stainless is included in this report to perhaps assist future experimentalists in the field. Several "standard" methods were employed but did not give the desired surface, scratch free and free of deformed metal.

After being loaded explosively, each sample was mounted in bakelite. The grinding was started using a 180 grit belt-driven paper of Si C. The hand grinding commenced with 320 grit Si C and progressed to the 400 A, 500 A, and 600 A grit Si C papers. All Si C papers were lubricated using a mixture of H<sub>2</sub>O and a commercially available liquid detergent. Grinding then proceeded to the 2/0 and 3/0 emery papers which were used dry. In each case grinding was done 90 degrees to the previous step and was continued until all previous scratches had been removed. This was checked microscopically before the next step was undertaken. The polishing technique was now started on the eight micron diamond wheel and progressed to the six micron and three micron diamond wheels. The last two polishing steps were accomplished using two grades of Al<sub>2</sub>O<sub>3</sub> suspension. As before, the sample was rotated 90 degrees from the direction on the previous wheel except on the last wheel where the sample was rotated at random. The sample was washed using a liquid detergent, rinsed in distilled water and alcohol and then dried with warm air between each operation. Considerable experimentation was done before a satisfactory etch was found. Since one end of each sample had been subjected to



tremendous loads, it was difficult to find an etch that would not preferentially attack the cold-worked end. A saturated solution of oxalic acid, used electrolytically, was found satisfactory. It was found that best results were obtained if etching was followed by a return to the last wheel. This procedure was continued until all deformed metal had been removed, as determined by a polarized light microscope.

Fig. 2 shows a detonated sample after etching.

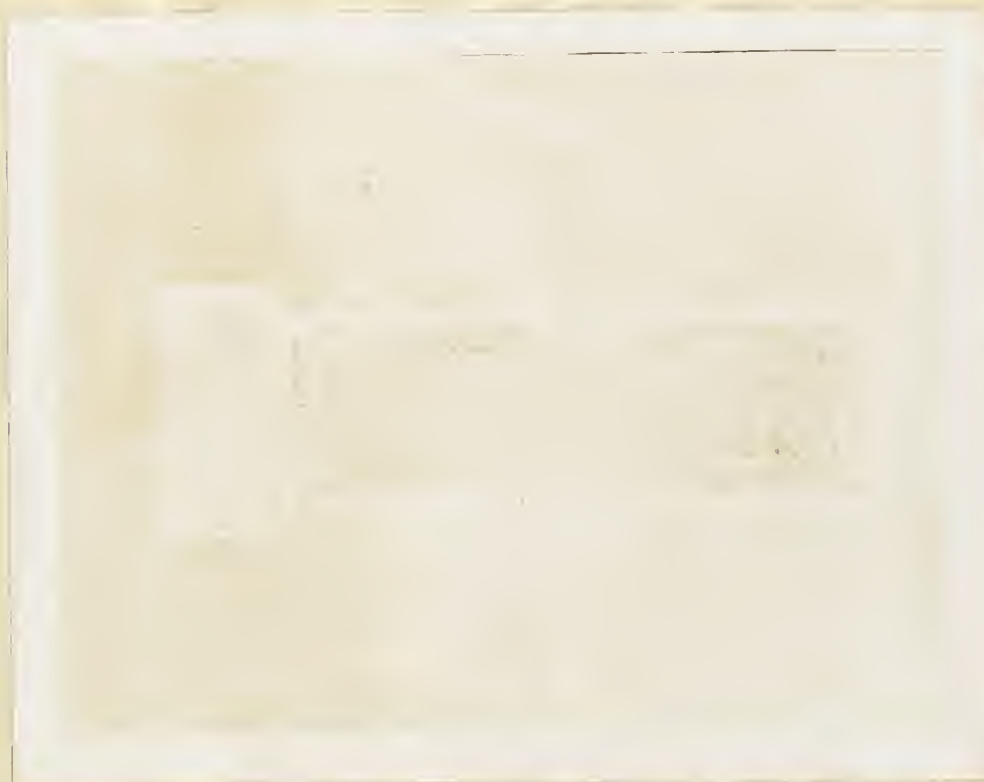


Fig. 2

497°C

7X



## 5. Discussion of Microstructures

All samples were examined at 200X using an American Optical metallograph. Fig. 3 through 9 show the microstructure obtained after polishing and etching as previously described. An examination of Fig. 4 through 9 indicates the temperature dependence of the results obtained. Most writers in the field indicate that slip lines are generally not visible if a sample has been polished and etched subsequent to deformation.<sup>11,12</sup> An examination of Fig. 4 through 10 reveals deformation lines within the crystal boundaries. The fact that these lines are readily observed after etching does not necessarily mean that they cannot represent slip. Recent work in Cambridge, England, has indicated that slip can be observed after etching.<sup>13</sup> Twinning is a possibility but further work with single crystals must be done before an exact statement can be made. Therefore, it seems advisable, at this time to refer to the lines solely as deformation lines. Fig. 3 is a photomicrograph of the crystal structure of the 18-8 stainless sample after annealing for one hour at 1050°C. Fig. 4 shows a sample after having been loaded at 97°C. This photograph was taken of the end which was farthest from the explosive. Very little, if any distortion has taken place; grain boundaries are sharply defined and the

<sup>11</sup>R. S. Williams and V. O. Homerberg, Principles of Metallography, McGraw-Hill Book Co., Inc., 1939

<sup>12</sup>Charles S. Barrett, Structures of Metals, pp. 339-340, McGraw-Hill Book Co., Inc., 1952

<sup>13</sup>D. G. Brandon and J. Nulting, The Metallography of Deformed Iron, Acta Metallurgica, Feb., 1959









Fig. 3

ONE HOUR ANNEALED

200X





Fig. 4

497°C. UNLOADED END

200X

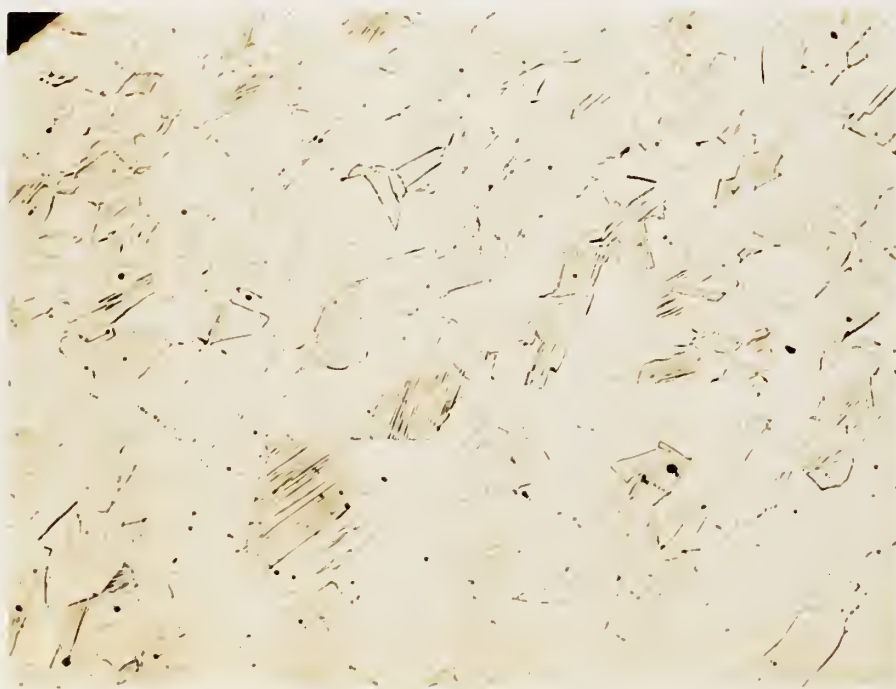


Fig. 5

497°C. LOADED END

200X



slight amount of deformation lines are confined to one plane. Fig. 5 is a photograph taken of the same sample as Fig. 4, however, this picture is of the loaded end of the sample. It is immediately obvious that much more distortion has been introduced. The grains are deformed as is evidenced by the deformation lines. An examination reveals the deformation lines have occurred along one plane. Fig. 6 and 7 are photographs of the unloaded and loaded ends respectively of the sample which was explosively loaded at 20°C. Fig. 6, of the unloaded end, shows little distortion present. A small amount of deformation is indicated by some deformation lines confined to one plane. Fig. 7 is of the cold worked or loaded end. Distortion has increased markedly and deformation is indicated by an increase in the number of deformation lines. However the deformation lines are still confined to one plane. Fig. 8 and 9 are of the unloaded and the loaded ends respectively of the sample explosively loaded at -190°C. Fig. 8 shows that the severe deformation has extended to the unloaded end. Numerous deformation lines are visible and three planes of deformation lines are present. Fig. 9 is of the explosively loaded end of the sample loaded at -190°C. Severe distortion is evidenced in all grains, grain boundaries are generally vague and indefinite. Severe deformation is indicated by numerous deformation lines. There are three planes of deformation lines evident in the structure.

Fig. 10 was taken at 1500X and is of the unloaded end of the sample explosively loaded at -190°C. This photograph shows a good case for twinning but is insufficient to







Fig. 6

20°C. UNLOADED END

200X



Fig. 7

20°C. LOADED END

200X





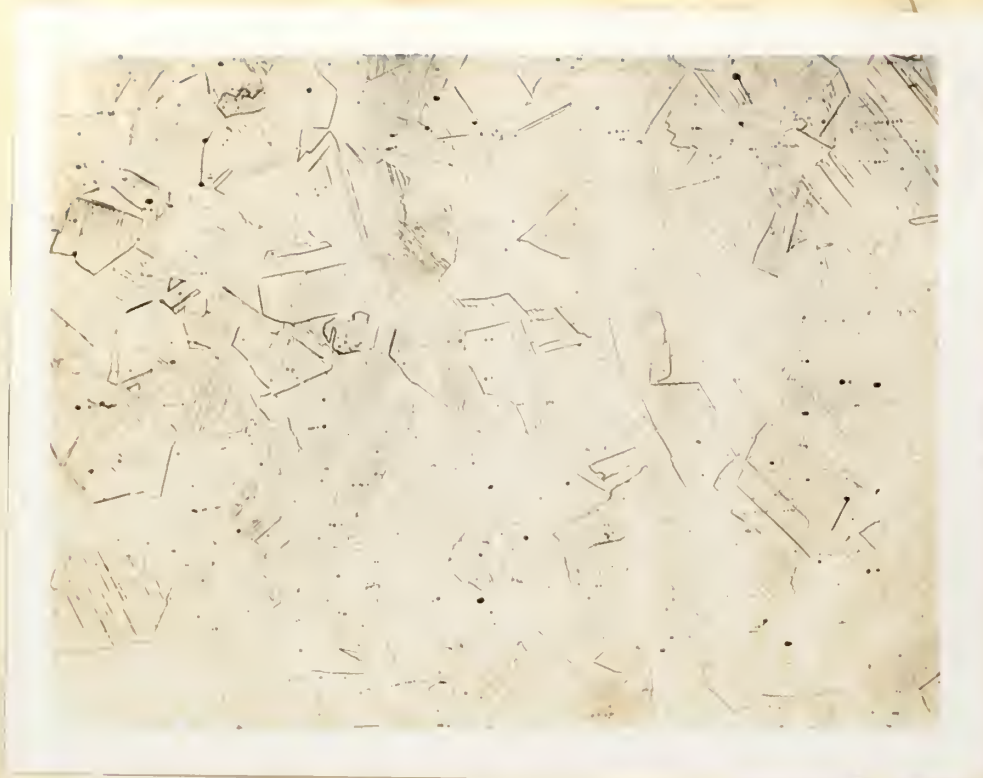


Fig. 8

-190°C. UNLOADED END

200X



Fig. 9

-190°C. LOADED END

200X



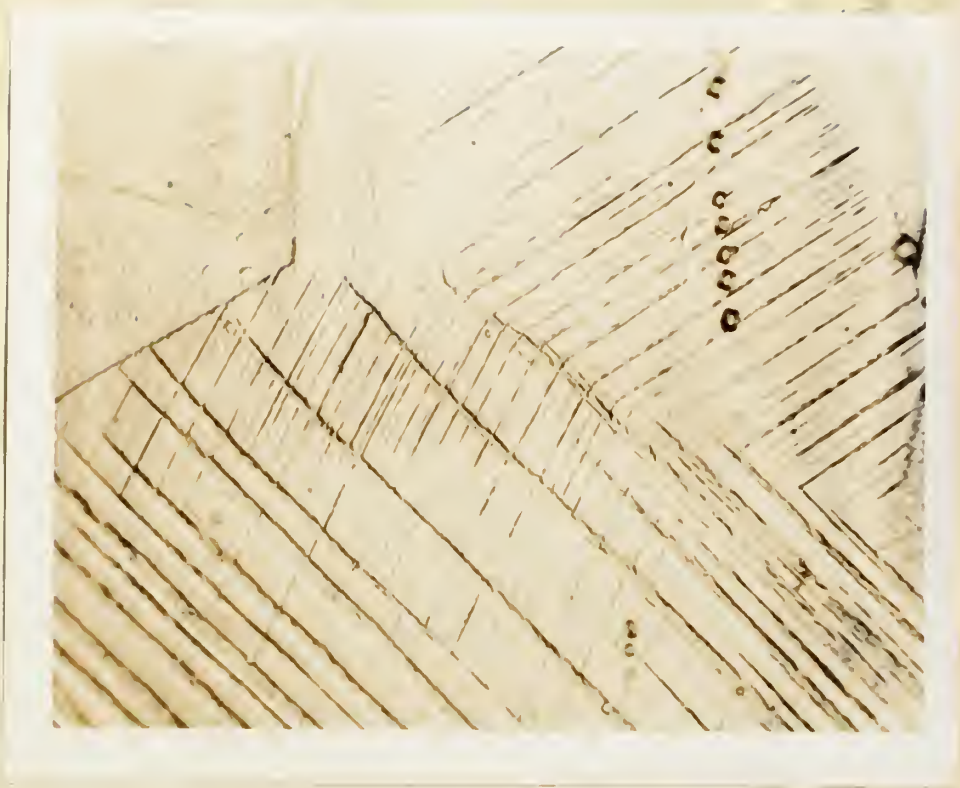


Fig. 10

-190°C. UNLOADED END

1500X



to constitute valid proof.

An examination of Fig. 4 through 10 indicates that the severity of the deformation lines and the number of deformation systems is definitely temperature dependent; that these factors increase with a decrease in temperature. The fact that different deformation systems are observed at different temperatures indicates that the alteration in shear strength with temperature is not uniform on all planes of the lattice.<sup>14</sup>

<sup>14</sup>Charles S. Barrett, Structure of Metals, pp. 351, McGraw-Hill Book Co., Inc., 1952





## 6. Discussion of X-ray Structure

X-ray diffraction is an important tool in that it can reveal details of internal structure of the order of  $10^{-8}$  cm. The mathematical basis for X-ray diffraction is Bragg's Law which can be stated as

$$n\lambda = 2d'\sin\theta$$

where  $n = 0, 1, 2, 3$  etc.,  $\lambda$  is the wavelength and  $d'$  is the spacing of the crystal planes. This law states the condition for reinforcement of all reflected rays. The Bragg law may be rewritten in the form

$$\lambda = 2d \sin\theta$$

where  $d = \frac{d'}{n}$

Since the coefficient of  $\lambda$  is now unity, a reflection of any order can be considered as a first order reflection from planes, real or fictitious, spaced at a distance  $1/n$  of the previous spacing.<sup>15</sup> The distance,  $d$ , between planes in a crystal, for the cubic system, can be determined by

$$d_{hkl} = \frac{a}{(h^2/k^2/l^2)^{1/2}}$$

where  $h, k, l$  refer to the Miller indices and  $a$  is the unit axial length of a crystal for the material under consideration. Combining this equation with Bragg's Law

$$\sin^2\theta = \frac{\lambda^2}{4a^2} (h^2/k^2/l^2)$$

This equation predicts, for a particular  $\lambda$  and a particular cubic crystal of unit size  $a$ , all the possible Bragg angles

<sup>15</sup>B. D. Cullity, Elements of X-ray Diffraction, pp.84, Addison-Wesley Publishing Co., 1956



at which diffraction can occur from the planes (hkl).

Diffraction directions are determined solely by the shape and size of the unit cell.<sup>16</sup>

In this investigation X-ray diffraction techniques were used for each sample detonated. The types of diffraction employed were the powder method and the back reflection method. Appendix II presents a sample calculation using the powder method and Appendix III a sample calculation using the back reflection method.

A sample of 18-8 stainless from the stock used in this experiment was placed on the Philips X-ray machine and back reflection technique was used to determine the best X-ray tube and filter combination to give minimum fluorescence consistent with sharply defined lines. In making a choice of the type of radiation to use it is important to have a characteristic radiation whose wavelength is shorter than the K absorption edge of the specimen under investigation or fluorescent radiation produced will fog the film. When monochromatic radiation is desired, a filter to remove the  $K_{\beta}$  radiation is necessary. A  $\beta$  filter is desired with K edge between  $K_{\alpha}$  and  $K_{\beta}$  emission wavelengths. The result of the initial experiments indicated that a chromium tube used with a vanadium filter gave the desired results. The emission and absorption wavelengths of Cr are given in Table II.

<sup>16</sup>Ibid, pp. 89



TABLE II

$\alpha_2$ (strong)	$\alpha_1$ (very strong)	$\beta_1$ (weak)	K absorption edge
2.29351 Å	2.28962 Å	2.0848 Å	2.0700 Å

The characteristic wavelength of Cr was determined to be 2.2910 Å by taking  $2/3 \alpha_2$  plus  $1/3 \alpha_1$ . The vanadium K absorption edge is 2.2690 Å. This filter reduces the intensity of  $K \beta$  to 1/600 of the  $K \alpha$  radiation.<sup>17</sup>

A piece of 18-8 stainless, taken from the stock used in this experiment, was cold worked using a file. Half of the filings were annealed for one hour at 1050°C. as were the rod samples used in this experiment. The other half of the filings were further cold worked by grinding under alcohol, using an agate mortar and pestle. The alcohol was used to prevent heating of the filings during the grinding operation. X-ray diffraction patterns were obtained from these two samples using the powder camera technique. In this manner, a standard interplanar spacing,  $d$ , could be determined both in the annealed and the cold worked cases. Annealed 18-8 stainless is of the austenitic ( $\gamma$  Fe) type; a non-magnetic, face centered cube. It was suspected that after being impulsively loaded at the three different temperatures, an appreciable amount of the austenitic phase would be transformed to ferritic ( $\alpha$  Fe) or magnetic phase which is of the body centered cubic type. Table III presents the results of the analysis of the powder X-ray taken of the stainless filings annealed at 1050°C. for one hour.

<sup>17</sup>Charles S. Barrett, Structure of Metals, pp. 58, McGraw-Hill Book Co., 1952





TABLE III

<u>Computed d Values (Å)</u>	<u>Observed d Values (Å)</u>	<u>Planes</u>
2.062	2.064	(111)
1.786	1.793	(200)
1.263	1.270	(220)

Also included in Table III are the theoretical d spacings for comparison purposes. The authors could find no published material giving d spacings for 18-8 stainless in the austenitic state. Barrett lists the unit cell distance a, for  $\gamma$  Fe as 3.571 Å, at 20°C.<sup>18</sup> This value was used in computing the theoretical d spacings using the formula

$$d_{hkl} = \frac{a}{(h^2/k^2/l^2)^{1/2}}$$

Barrett also lists the permitted (hkl) values for cubic crystals and these were used in the calculations.<sup>19</sup> Examining Bragg's equation

$$\lambda = 2d \sin \theta$$

it is noted that the minimum d value observable occurs when  $\sin \theta = 1$  and corresponds to a d value of  $\lambda/2$ . In the case of chromium radiation this would be a d value equal to 1.145 Å. Values of d less than this were not listed since they could not be observed on the X-ray film. An examination of Table III shows that there is very good agreement between the theoretical and measured values. This confirms that in the annealed state, 18-8 stainless is of the austenitic or  $\gamma$  Fe type. Table IV lists the results of the analysis of the X-ray diffraction taken of the cold worked filings.

<sup>18</sup>Ibid, App. IX, pp. 647

<sup>19</sup>Ibid, App. VII, pp. 642





TABLE IV

<u>Computed d Values (Å)</u>	<u>Observed d Values (Å)</u>	<u>Identification</u>
2.062	2.071	(111) $\gamma$
2.027	2.031	(110) $\alpha$
1.786	1.801	(200) $\gamma$
1.263	1.269	(220) $\gamma$
1.170	1.171	(211) $\alpha$

The computed values listed in Table IV were obtained from X-ray Powder Data File Cards for  $\alpha$  Fe prepared by the American Society for Testing Materials, The American Crystallographic Association, The (British) Institute of Physics, and The National Association of Corrosion Engineers. An examination of Table IV shows that only a portion of the filings were transformed to the  $\alpha$  Fe or ferritic phase. This was a sufficient transformation to induce magnetism in the filings. The measured d values listed in Table IV are in quite good agreement with theoretical  $\gamma$  Fe and  $\alpha$  Fe d spacings. These d spacings were used to check the existence of either phase during this investigation.

A sample of 18-8 stainless steel which had been annealed for one hour at 1050°C., mounted in bakelite, polished and etched sufficiently to eliminate grinding effects, was placed on the Hilger Research X-ray diffraction unit. Each diffraction was conducted using 35 kv and 10 ma. A back reflection exposure was obtained using chromium radiation filtered by vanadium. The film was rotated continuously for three hours and a 0.4 mm collimator was used. The d spacing for this piece of 18-8 stainless was found to be 1.270 Å, (110) plane for  $\gamma$  Fe, which checks very well with the



previous calculations for 18-8 in the annealed or austenitic condition. Fig. 11 is a picture of the results obtained from this exposure.

The next back reflection X-ray diffraction was made of the piece of 18-8 stainless which had been loaded explosively at  $497^{\circ}\text{C}$ . Fig. 12 shows the results of this exposure. The quadrants marked 2 and 4 are of the end of the sample which was <sup>un</sup>loaded and the quadrants marked one and three are of the opposite end. Although a ferrite line is not visible, it can be seen by the intensity of the lines that the loaded end shows less austenite than does the other end although this difference is slight and Fig. 12 does not differ from Fig. 11 appreciably. The d value for the unloaded end was found to be  $1.272 \text{ \AA}$ , the (110) plane of the  $\gamma$  iron phase, which is in good agreement with the d value found for the austenitic type stainless. The d value for the loaded end was found to be  $1.272 \text{ \AA}$  indicating no detectable phase change at  $497^{\circ}\text{C}$ .

Fig. 13 is the result of the back reflection diffraction of the sample of 18-8 stainless which had been loaded at  $20^{\circ}\text{C}$ . Quadrant shielding was employed in Fig. 13; opposite quadrants being of the same end of the sample. Referring to Fig. 13, quadrants marked two and four are of the end of the sample which was loaded explosively. Quadrants marked one and three are of the opposite end of the sample. The d spacing of the unloaded end of the sample depicted in Fig. 13 (quadrants three and <sup>one</sup>four) is  $1.270 \text{ \AA}$  which is the (110) plane of austenitic type or annealed stainless. Here, again,



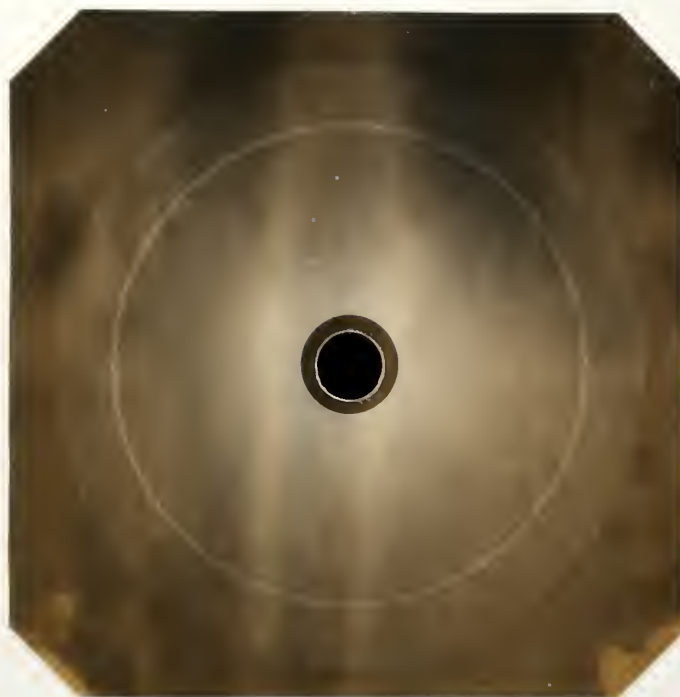


Fig. 11      One Hour Annealed      X-ray



Fig. 12      Sections 1 & 3-Loaded End X-ray  
                  Sections 2 & 4-Unloaded End  
                  497°C.







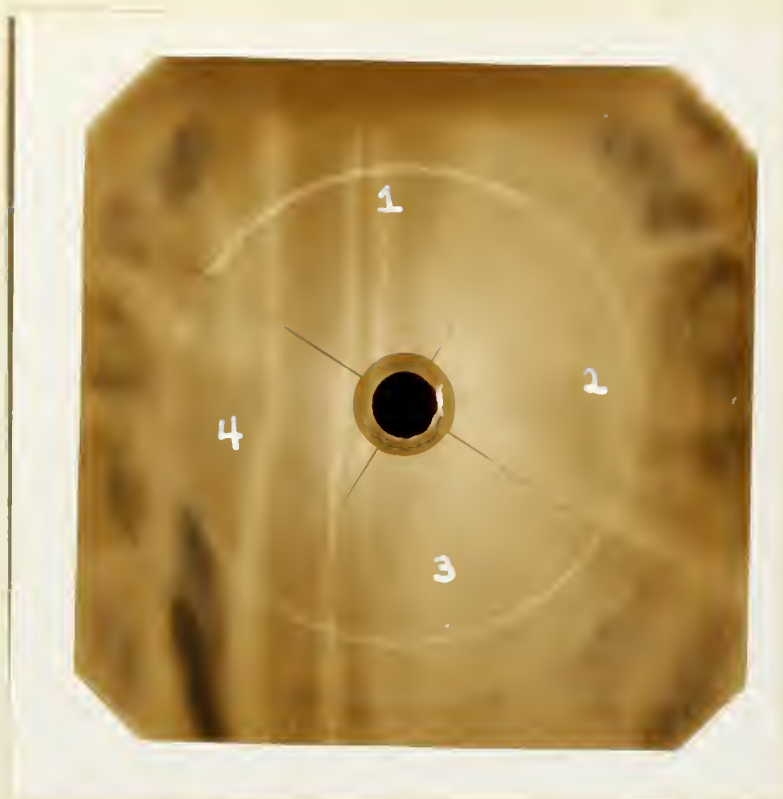


Fig. 13      / 20°C.      X-ray  
Sections 1 & 3-Unloaded End  
Sections 2 & 4-Loaded End



there is no evidence of a ferritic type transformation. However, referring to Fig. 13, quadrants marked two and four, two distinct diffraction arcs can be seen without difficulty. The  $d$  value for the outer arc is  $1.271 \text{ \AA}$  which is plane (110) of the austenitic phase. The  $d$  value for the inner circle is  $1.173 \text{ \AA}$  which agrees very well with the  $d$  value for the (211) plane of the ferritic phase as shown in Table IV. Thus in the case of the sample loaded explosively at  $\neq 20^{\circ}\text{C.}$ , a definite phase change has occurred in the loaded or cold worked end. An examination of the intensity of the arcs in quadrants two and four of Fig. 13 indicates that the austenitic or  $\gamma$  phase still predominates.

The specimen of 18-8 stainless steel loaded at  $-190^{\circ}\text{C.}$  was then studied by the same X-ray method. Fig. 14 is a print of the results obtained from the diffraction. Quadrants marked two and four are of the explosively loaded end. Quadrants marked one and three are results obtained using the unloaded end of the sample. In this sample a marked phase change can be detected. Referring to Fig. 14, the outer arc of quadrants two and four is too faint to be measured. The  $d$  value of the inner arc was found to be  $1.171 \text{ \AA}$  which is the (211) plane of the ferritic or  $\alpha$  phase. The  $d$  value of the outer arc in quadrants one and three was found to be  $1.270 \text{ \AA}$  which is the (110) plane of the austenitic or  $\gamma$  phase. Thus a marked phase change is obvious in the sample loaded at  $-190^{\circ}\text{C.}$  The loaded end of the sample is practically all of the ferritic or  $\alpha$  phase and the opposite end is predominantly of the austenitic or  $\gamma$  phase.





Fig. 14      -190°C.      X-ray  
Sections 1 & 3-Unloaded End  
Sections 2 & 4-Loaded End





although some change to the ferritic phase has occurred as can be seen from the faint inner arcs in Fig. 14, quadrants one and three.

An attempt was made to show the decrease in the amount of austenite present, as indicated by Fig. 15. The Philips X-ray unit was used, focussing on the  $1.270 \text{ \AA}$  line of austenitic phase and obtaining back reflection diffractions of each of the samples by rotating both the sample and the film in opposite directions for one hour of exposure. The quadrants marked one, two, three and four are of the one hour annealed,  $-190^{\circ}\text{C.}$ ,  $\nearrow 97^{\circ}\text{C.}$  and  $\nearrow 20^{\circ}\text{C.}$  samples respectively. The quadrants two, three and four are diffractions of the explosively loaded ends of the samples. The intensity of the lines indicates a definite decreasing amount of austenite or face centered phase as the temperature was lowered.

Fig. 16 shows the results obtained when this same procedure was used by focussing on the  $1.171 \text{ \AA}$  line. The one hour annealed sample was replaced by a sample of commercially pure annealed iron. Quadrant number one is the pure iron diffraction pattern and quadrants two, three and four are the patterns obtained from the loaded ends of  $\nearrow 97^{\circ}\text{C.}$ ,  $\nearrow 20^{\circ}\text{C.}$  and  $-190^{\circ}\text{C.}$  samples respectively. Each sector was exposed for a period of two hours and the composite photograph indicates an increasing amount of ferrite as temperature decreases. The exposure time was sufficiently long enough to permit a trace of  $K_{\beta}$  radiation to appear on the pure iron pattern (sector one, outer-most line). Furthermore, the doublet was resolved. The angle of reflection in this case was  $25^{\circ}$  while







Fig. 15

Composite

X-ray

Section 1-One Hour Annealed  
 Section 2-Loaded End  $-190^{\circ}\text{C}$ .  
 Section 3-Loaded End  $+97^{\circ}\text{C}$ .  
 Section 4-Loaded End  $+20^{\circ}\text{C}$ .





Fig. 16      Composite      X-ray

Section 1-	Annealed Iron
Section 2-	Loaded End $+97^{\circ}\text{C.}$
Section 3-	Loaded End $+20^{\circ}\text{C.}$
Section 4-	Loaded End $-190^{\circ}\text{C.}$



in the austenite the reflection angle was  $51^{\circ}18'$ . Due to the limitation of film size the  $K_{\alpha}$  doublet was not resolved in Fig. 15. Section two indicated no transformation for the exposure time used and in section three a trace is apparent. In section four a wide unresolved line was obtained.

Both Fig. 15 and 16 indicate a broadening or diffusion of diffraction lines as the temperature decreased. This is in agreement with theory that when an annealed metal or alloy is cold worked, its diffraction lines become broader. This broadening of the diffraction lines may result from variation in lattice spacing in different parts of the crystals or from breaking up of the crystals into very small crystallites of differing orientation.<sup>20</sup>

Several attempts were made to show the existence of preferred orientation. No positive results were obtained from this investigation.

<sup>20</sup>William Hume-Rothery, *Electrons, Atoms, Metals and Alloys*, pp. 271, Metal Industry, 1955.

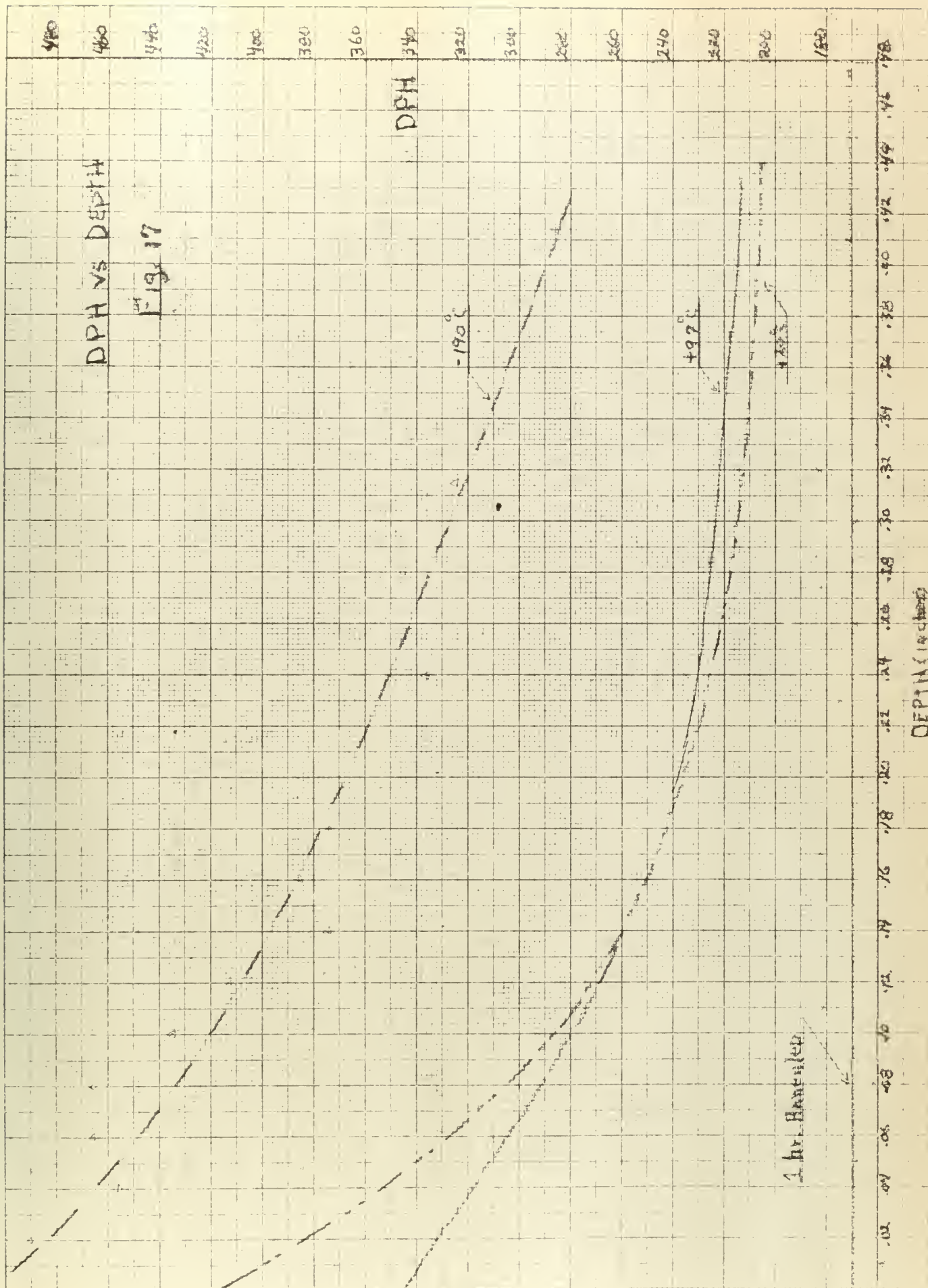




## 7. Hardness

Microhardness profiles were obtained of samples loaded at each temperature and compared to an annealed sample that was not loaded. The Bergsman Microhardness Tester as adapted to the American Optical Metallograph by E. W. LaRocca was used for this part of the investigation. Each sample was tested about every .010 inch. The diamond pyramid hardness (DPH), versus depth from the impulsively loaded end is presented in Fig. 17. An examination of this graph shows that, in each sample which had been loaded, the hardness is greatest at the loaded end and decreases toward the unstressed end. It is also apparent that hardness increases with a decrease in temperature at the impulsively loaded end.







## 8. Conclusions

Type 304, 18-8 stainless steel, when quenched from a temperature of 1050°C. is austenitic, and has the structure of iron, i.e., face-centered cubic. This structure is metastable and as such does not represent an equilibrium condition. When cold worked a portion of the material converts to a more stable form, the body-centered cubic. This phase change occurs when the material is explosively loaded, and can occur in a period measured in microseconds. After being explosively loaded deformation is evidenced by varying degrees of deformation. The amount of phase change and the severity of deformation are both a direct function of temperature, increasing as the temperature decreases. Hardness decreases with distance from the loaded end of the samples, and increases with a decrease in temperature at the loaded end.

The desirability of stainless steel is partly due to its anti-corrosion and anti-magnetic characteristics. These characteristics are of particular interest in the field of missiles and air craft. Under explosive loading or impact, stainless steel loses these desirable characteristics with the formation of ferrite or martensite.

It is recommended that further study in the field be done using single crystals so that individual grains can be examined by diffraction methods for better understanding of 1. orientation and 2. phase relationship. It is also recommended that further investigation of 1. a greater temperature range and 2. various amounts of loading be included.





## BIBLIOGRAPHY

1. Charles S. Barrett, Structure of Metals, McGraw-Hill Book Co., Inc., 1953.
2. John S. Rinehart and John Pearson, Behavior of Metals Under Impulsive Loads, The American Society for Metals, 1954.
3. B. D. Cullity, Elements of X-ray Diffraction, Addison-Wesley Publishing Co., Inc., 1956.
4. William Hume-Rothery, Electrons, Atoms, Metals and Alloys, Metal Industry (British), 1955.
5. Carl A. Zapffe, Stainless Steels, The American Society For Metals, 1949.
6. J. R. Vilella, Metallographic Technique For Steel, The American Society for Metals, 1938.
7. Gilbert E. Doan and Elbert M. Mahla, The Principles Of Physical Metallurgy, McGraw-Hill Book Co., Inc., 1941.
8. Ernest E. Thum, The Book Of Stainless Steels, The American Society For Metals, 1935.
9. George L. Kehl, The Principles Of Metallographic Laboratory Practice, McGraw-Hill Book Co., Inc., 1943.
10. Taylor Lyman Metals Handbook, 1948 Edition, American Society For Metals, 1954.
11. E. W. LaRocca, Adaption Of Bergsman Microhardness Tester To American Optical Metallograph, The Review Of Scientific Instruments, Vol. 26, No. 6, pp. 590-591, June, 1955.
12. N. F. M. Henry, H. Lipson and W. A. Wooster, The Interpretation of X-ray Diffraction Photographs, D. Van Nostrand Co., Inc., 1951.
13. Iu. N. Riabinin, Certain Experiments On Dynamic Compression Of Substances, Soviet (Tech.) Physics, Vol. 1, No. 12 (1956), translation by Am. Inst. Phys.
14. H. Trach Hall, Ultrahigh-Pressure Research, Science Vol. 128, No. 3322, 29 Aug., 1958.
15. E. O. Hall Twinning And Diffusionless Transformations In Metals, Butterworths Scientific Publication, 1954.
16. R. S. Williams and V. O. Homerberg, Principles Of Metallography, McGraw-Hill Book Co., Inc., 1939.



17. D. G. Brandon and J. Nulting, The Metallography Of Deformed Iron, Acta Metallurgica, Feb., 1959.



## APPENDIX I

### ANALYSIS AND TESTS

#### 1. DESCRIPTION OF MATERIALS

a) Type 304 S. S. Annld & C. D.  $\frac{1}{4}$  in. Rd.

#### 2. CHEMICAL ANALYSIS

Manufacturer; Allegheny

Heat No.....	B-64973	Nickel.....	8.75%
Carbon.....	.050%	Chromium.....	18.42%
Mang.....	.44%	Moly.....	.15%
Phos.....	.021%	Copper.....	.18%
Sulphur.....	.008%		
Silicon.....	.35%		

#### 3. MECHANICAL PROPERTIES

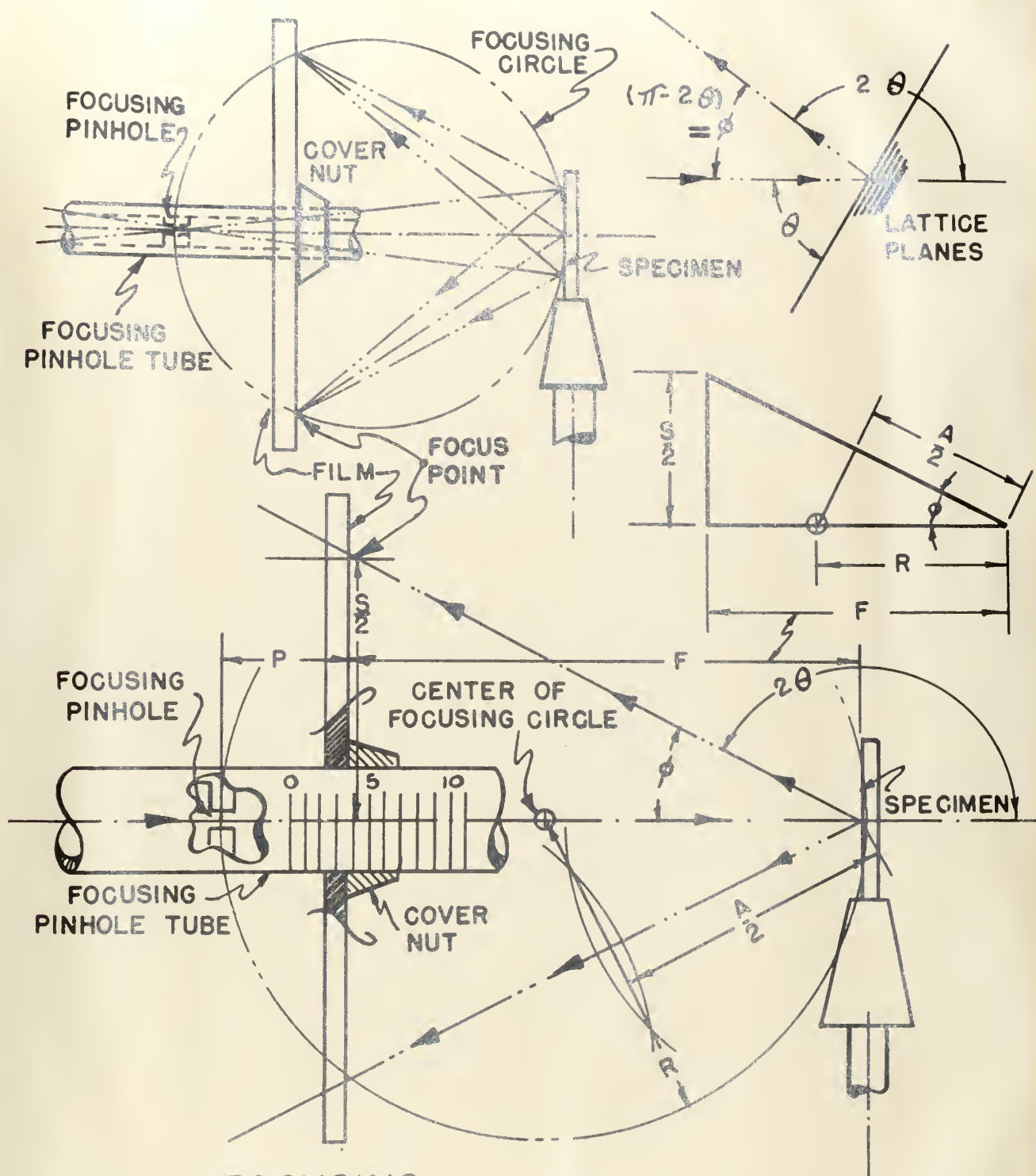
Tensile Strength.....	102,000 lbs./sq. in.
Yield.....	81,000 lbs./sq. in.
Elongation.....	54%
Reduction of Area.....	68%











## BASIC FOCUSING GEOMETRY

APPENDIX III



### APPENDIX III

#### SAMPLE CALCULATIONS FOR FLAT PLATE B R

S = Radius of circle on film (Fig. 11, one hour annealed)  
= 31.2 mm.

R = Distance from film to sample = 25.0 mm.

From basic geometry;

$$\tan (180-2\theta) = 1.248 = S/R$$

$$\theta = \frac{180 - 51^{\circ}18'}{2} = 64^{\circ}21'$$

From Bragg's Law;

$$\hat{d} = \frac{\lambda}{2 \sin \theta} = 1.270, (110) \text{ for } \gamma \text{ iron}$$

where  $\lambda = 2.291$  for chromium









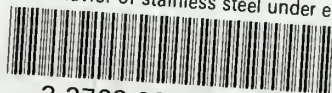






thesA718

The behavior of stainless steel under ex



3 2768 002 01251 0  
DUDLEY KNOX LIBRARY